

Supporting Information

© Wiley-VCH 2013

69451 Weinheim, Germany

**Colloidal Clusters by Using Emulsions and Dumbbell-Shaped Particles:
Experiments and Simulations****

Bo Peng, Frank Smalenburg,* Arnout Imhof, Marjolein Dijkstra, and Alfons van Blaaderen**

anie_201301520_sm_miscellaneous_information.pdf

Table of contents

Materials	S2
Particles preparation	S2
Density Gradient Separation	S4
Sample Observation	S4
Simulation Methods	S4
Particles at Interface	S8
Clusters of Single Spheres	S9
Clusters from Symmetric Dumbbells	S11
Clusters from Asymmetric Dumbbells	S12
Supplementary References	S13

Materials and Methods

Materials

Methyl methacrylate (MMA, Aldrich, chemical grade) was passed over an inhibitor removal column (Aldrich). After the inhibitor had been removed, MMA was stored in a refrigerator at 4 °C and not longer than one month. Azo-bis-isobutyronitrile (AIBN, Janssen Chimica) was re-crystallized from ethanol before use. Ethylene glycol dimethacrylate (EGDMA, Sigma-Aldrich, chemical grade) was used as the cross-linking agent. Polyvinylpyrrolidone (PVP, Fluka, chemical grade) with an average molecular weight of 360,000 g/mol (K-90) was used as the stabilizer. Hydroquinone (Fluka, chemical grade) was used as the inhibitor. Sorbitan monooleate (Span 80, Aldrich, chemical grade), methanol (Biosolve, chemical grade), dodecane (Aldrich, $\geq 99\%$) and glycerol (Sigma-Aldrich, $\geq 99.5\%$) were used as supplied. Deionized water was used in all experiments and was obtained from a Millipore Direct-Q UV3 reverse osmosis filter apparatus.

Particles Preparation

The spherical PMMA (poly methyl methacrylate) particles were prepared by dispersion polymerization following an adaption that is mentioned in supplementary ref. 1 (SR-1) and had a radius of 0.69 μm and polydispersity of 3%. In detail, the solvent mixture of methanol (30.6 g) and water (6.14 g) containing 4.1 wt% PVP stabilizer was prepared first. Then, two thirds of this mixture, all of the monomer (2.5 g of MMA) and initiator (0.025 g of AIBN) were blended homogeneously under constant stirring at ~ 200 rpm in a 250 ml flask. Nitrogen was bubbled through this mixture for at least 30 min. Then, the flask was immersed in a silicon oil bath and maintained at 55 °C under stirring at 100 rpm. 1 wt% (based on monomer mass) of cross-linker was mixed with the remaining one third of solvent-stabilizer mixture, and slowly fed into the flask from the beginning of the reaction at a constant addition rate for 10 h. After the addition was complete, the reaction mixture was maintained at 55 °C for 24 h before cooling down to room temperature. The obtained particles were

rinsed three times with methanol, and then three times with de-ionized water. Finally, they were dispersed in de-ionized water.

The asymmetric and symmetric dumbbells were fabricated by an ‘over-swelling’ method as reported in SR-2. Firstly, the cross-linked seed PMMA particles were prepared by dispersion polymerization in a methanol and water mixture, as described above (also see SR-1), then the swelling of seed particles took place in aqueous solution which contained swelling monomer droplets (MMA) in the presence of the initiator AIBN and the steric stabilizer PVP (1 wt% based on total mass), the second aqueous solution contained seed particles (~ 0.7 wt%) stabilized by PVP (1 wt% based on total mass). After 18 h of gentle stirring (< 100 rpm), the cross-linked seed particles over-swell and phase separate to form a protrusion. Re-polymerization was carried out at $70\text{ }^{\circ}\text{C}$ under an N_2 atmosphere for 8 h before cooling. The radius ratio could be precisely controlled by varying the amount of monomer (MMA, for details see SR-2). The final particle suspension was washed four times with de-ionized water using a centrifuge to remove the second nucleation and impurities. In our experiments, we used symmetric dumbbells with a radius of $0.71\text{ }\mu\text{m}$ (polydispersity of 2.2 %) and a contact angle of $54^{\circ}\pm 3^{\circ}$, and asymmetric dumbbells with R_s (radius of seeds in asymmetric dumbbells) of $0.71\text{ }\mu\text{m}$ (polydispersity of 2.3%), R_p (radius of polymer protrusion) of $0.52\text{ }\mu\text{m}$ (polydispersity of 3.7%) and a contact angle of $48.5^{\circ}\pm 3^{\circ}$. SEM images of the particles obtained are shown in Supplementary Figure 1 (SF-1) a-c.

Clusters of these three particles were produced from water-in-oil emulsions. 1 ml of an aqueous dispersion of particles (1 wt% based on water mass) was mixed with 20 ml of dodecane with a stabilizer (Span 80, 0.5 wt% based on the dodecane mass) and emulsified by shearing at 3500 rpm for 3 minutes. Clusters were formed by self-organization of the spherical or non-spherical particles during the slow evaporation of water at $90\text{ }^{\circ}\text{C}$ for 3 h. The obtained clusters were carefully washed with hexane (sedimented at 1 g for 12 h and re-dispersed under a ~ 300 rpm stirring) and dried under N_2 fluid. Ultimately, the clusters were re-dispersed in water (20 ml) by gently shaking by hand.

Density Gradient Separation

A linear density gradient method was performed by using two solvents with different densities and viscosities, in this case water and glycerol. A homemade two-column type gradient forming device was used to prepare a 30 wt% -70 wt% glycerol aqueous solution. 10 ml of the cluster suspension was loaded on top of 100 ml of linear density gradient and centrifuged (Hettich Rotina 46 S) at 2000 rpm for 12 minutes. Isolated cluster bands that consisted of clusters of equal numbers of particles were formed. These fractionated uniform clusters were picked out by a pipette and glycerol was rinsed out by repeated centrifugation (at 1 g). Samples were finally dispersed in water for further characterization.

Sample Observation

In order to better understand the state of dispersion of the particles at the water-oil interface, we observed the sample with an optical microscope (Leica) equipped with a 63 \times objective at room temperature. After the evaporation and SA procedure had finished and the clusters washed, the detailed configuration of the clusters collected on a glass slide was determined by performing scanning electron microscopy (SEM) with a FEI Phenom scanning electron microscope. Samples were dried onto a glass slide at room temperature and sputter-coated with a layer of gold (Au) of 5 nm. None of the images shown were post-processed.

Simulation Methods

We tried to mimic the behavior of the colloidal particles in an emulsion droplet during the evaporation of the solvent by a simplified two-step procedure. In the experimental setup, the particle-particle and particle-wall interactions are difficult to determine and will probably change during the evaporation process. We assumed that the particles were confined to a spherical cavity that shrinks during the evaporation of the droplets. As a first approximation, we modeled the particles and the droplet interface by hard interactions. As a result, no deformations of the wall from its spherical shape occurred, which is justified in the first stage of the evaporation process, *i.e.*, before packing constraints become important.

We simulated both spherical and dumbbell particles. In all cases, our unit of length was taken to be R_s , the diameter of the largest sphere size. The dumbbells are modeled as two partially overlapping hard spheres with diameter ratio $q = R_p / R_s$, at a fixed distance d ($d = \sqrt{R_s^2 + R_p^2 - 2R_s R_p \cos \theta}$, for details see SF-1d) between the centers. For both spherical and dumbbell particles, the center of mass of each sphere was confined to a spherical simulation box with hard walls. During the simulations, the pressure was slowly increased from $P^* = PR_s^3 / k_B T = 1$ to 20 to mimic the evaporation of the droplet. At $P^* = 20$, the particles no longer have enough freedom of movement to rearrange, but still vibrate. To fix the structure, the pressure was then rapidly increased to $P^* = 100$, effectively leading to a fully jammed state.

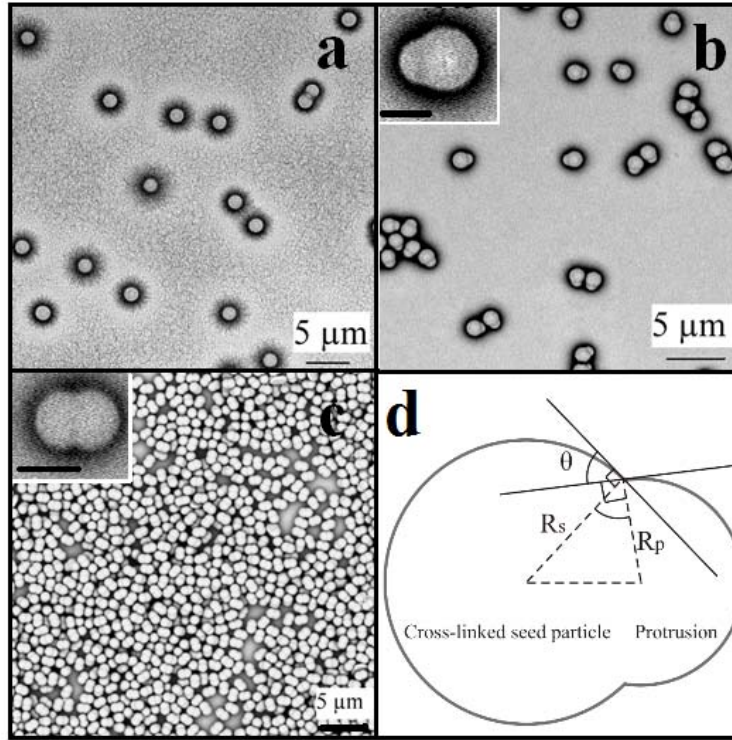
In our simulations, we considered two different regimes for the particle wettability. In the non-wetting regime (contact angle $\cos \theta = 1$), the particles could move freely within the spherical cavity under the constraint that the particles did not overlap with each other or the droplet interface. We chose to also investigate this limit for two reasons: first, to see how much it matters if the particles are confined to an interface or not, but also because this limit has been observed for instance for sterically stabilized PMMA particles in apolar solvents (see *e.g.* SR-3, 4). Additionally, this limit may be relevant when there are so many particles that they cannot occupy the surface area, a limit not covered experimentally in this paper (see *e.g.* SR-5). For finite wettability ($-1 < \cos \theta < 1$), the particles are attached to the droplet interface by a strong adsorption free energy, for particles used in the present study at least thousands of $k_B T$ (also see SF-2), [30] which we modeled by confining the center of mass of the particles to a thin spherical shell with thickness $d_s = 0.1R_p$ at the droplet surface, where R_p is the diameter of the smallest sphere in the system. We found that the final structure of the cluster is not affected by the shell thickness d_s , provided that $d_s \ll R_p$.

Manoharan *et al.* [8] suggested that after reaching this spherical packing stage, further evaporation of the droplet induces a reorganization of the particles due to the attractive Van der Waals interactions, which reduces the second moment of the mass distribution in the system. To model the second stage of the evaporation process, we used the jammed spherical clusters obtained from the spherical

compression simulations, removed the spherical confinement, and used a standard Monte Carlo scheme to minimize M_2 . In this simulation, the total energy of the system was taken to be proportional to M_2 , with a dimensionless proportionality constant α that is increased slowly to anneal the cluster to a local potential energy minimum:

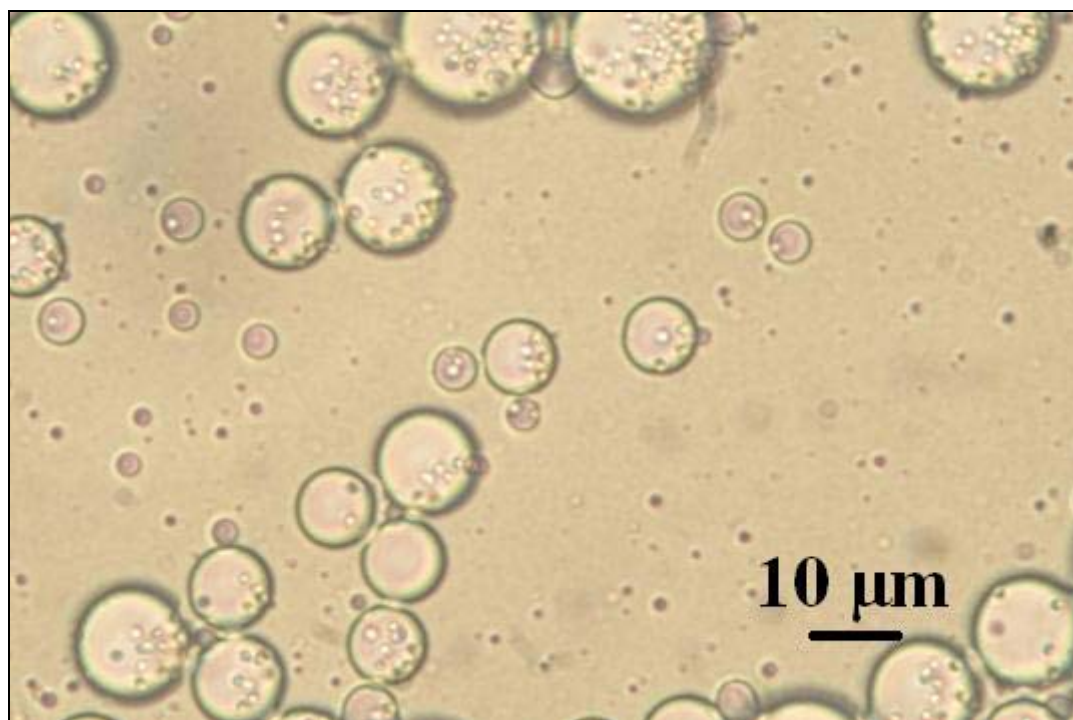
$$\beta U(r_s^N) = \alpha \sum_{i=1}^N m_i |r_i - r_0|^2 / R^2 \quad (\text{SE.1})$$

with $\beta = 1 / k_B T$, k_B Boltzmann's constant, T the temperature, R the diameter of the largest sphere size, and N the number of spheres in the cluster. In the case of dumbbell particles, each sphere was counted separately in the summation. The (dimensionless) mass m_i is only important if multiple sphere sizes appear in the system, and was taken to be 1 for the largest sphere size in the system. The strength of the potential α was increased from 100 to 1000, at which point no further reorganization is observed. The system is then quenched at $\alpha = 10000$ to remove any further vibrations. For the results presented below, both the compression and annealing parts of the simulation consisted of $8 \cdot 10^6$ Monte Carlo cycles. We also performed simulations with lower compression and annealing rates, but found similar results for the final clusters.



Supplementary Figure 1. Scanning electron microscopy (SEM) images and schematic model image of the three different colloidal building blocks. (a) SEM micrograph of the spherical building blocks (radius of $0.69\ \mu\text{m}$ and polydispersity of 3%). (b) SEM micrograph of the asymmetrical dumbbell particles ($R_s = 0.71\ \mu\text{m}$ 2.3% in polydispersity; $R_p = 0.52\ \mu\text{m}$, 3.7% in polydispersity; and $\theta = 49^\circ \pm 3^\circ$); the scale bar in the inset image is $1\ \mu\text{m}$. (c) SEM micrograph of symmetric dumbbell particles ($R_s = 0.71\ \mu\text{m}$, 2.2% in polydispersity and $\theta = 54^\circ \pm 3^\circ$); the scale bar in the inset image is $2\ \mu\text{m}$. (d) Schematic diagram of dumbbell particles; where R_s and R_p are the radius of the seed and protrusion part of the dumbbell, respectively, and θ is the contact angle of the dumbbell.





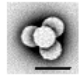




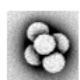



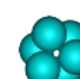


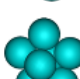

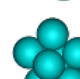
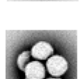

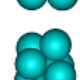
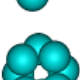
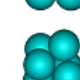
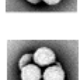
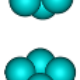
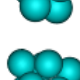
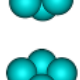
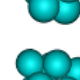
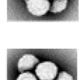
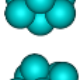
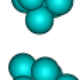
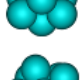
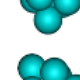
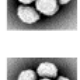
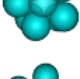
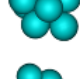
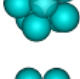
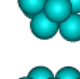
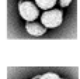
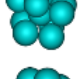
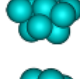
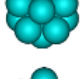
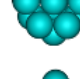
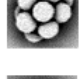

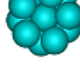




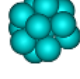

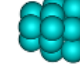

Particles at Interface



Supplementary Figure 2. Optical microscopy image of the asymmetric dumbbells particles which were all found adsorbed, as expected, at the water/oil interface (before heating), not dispersed in the oil.

Clusters of Single Spheres

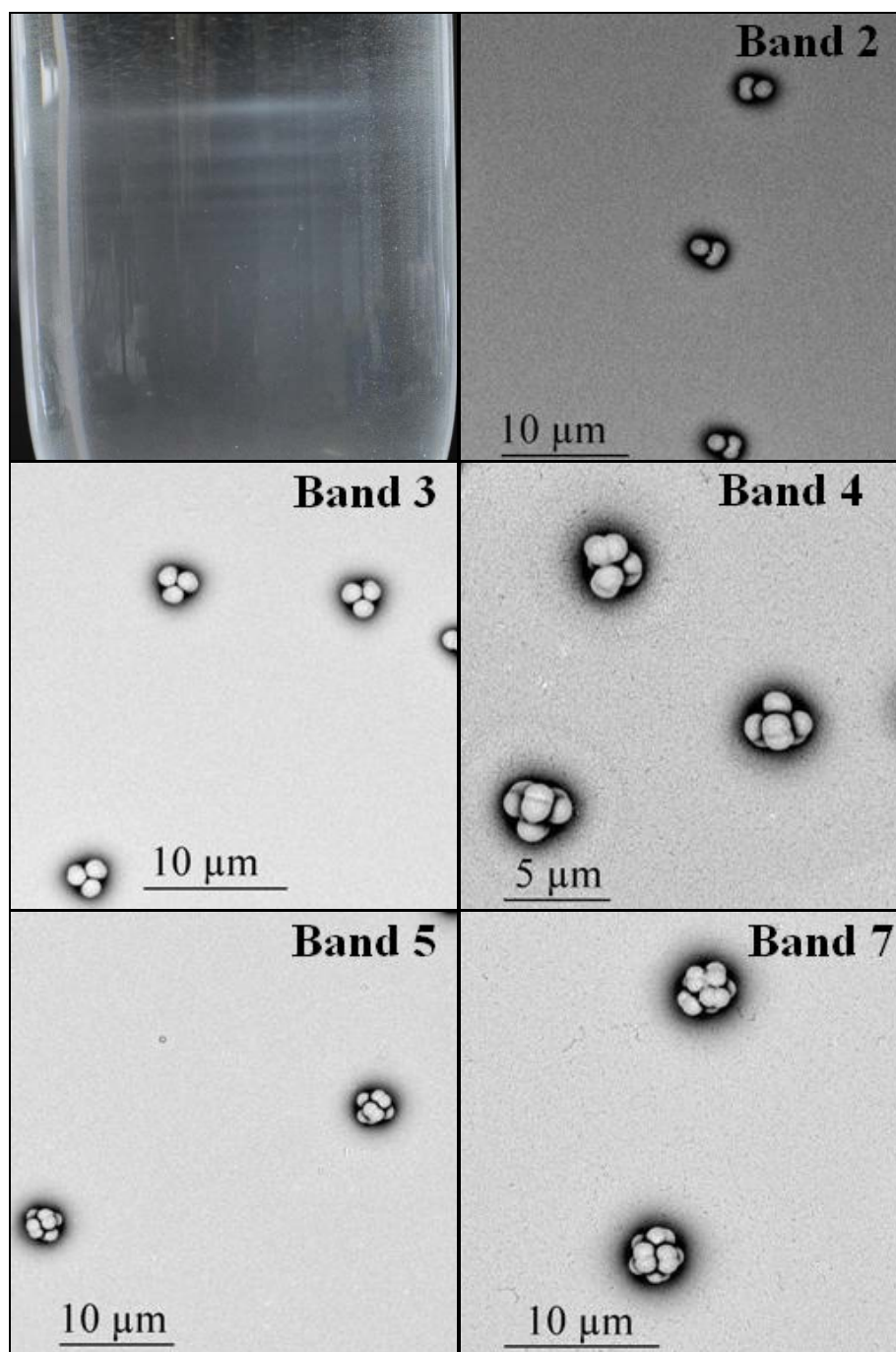
As a test for our method, we first applied it to clusters of spherical particles, with cluster sizes $4 \leq N \leq 14$. The spherical PMMA (poly methyl methacrylate) particles were prepared by dispersion polymerization following an adaption mentioned in ref. 10 and had a radius of $0.69 \mu\text{m}$ and polydispersity of 3% (see Supporting Fig. 1a, SI-1a). In simulations, we present the results of the packing before and after minimizing M2 for both wettable and non-wettable particles, as well as the corresponding experimental images, in Supporting Tab. 1 (ST-1). As expected, the experimentally observed clusters $N \leq 12$ match with the simulated wettable particles after M2 minimization. For larger clusters ($N > 12$), no clear match between simulations and experiments can be found. Nonetheless, it is clear that for sufficiently small clusters, our method provides a good indication of the types of structures that can be expected in clusters formed by evaporation of emulsion droplets with spherical particles.

N	Non-wettable		Wettable		Observed
	before	after	before	after	
4	a 	a 	a 	a 	a 
5	a 	b 	a 	b 	b 
6	a 	a 	a 	a 	a 
7	a 	b 	a 	b 	b 
8	a 	b 	a 	b 	b 
9	a 	b 	a 	b 	b 
10	a 	b 	a 	b 	b 
11	a 	b 	c 	d 	d 
12	a 	a 	b 	b 	b 
13	a 	b 	c 	d 	e 
14	a 	b 	c 	d 	e 

Supplementary Table 1. Structures found from simulations of spherical particles in evaporation droplets, and experimental results. The first column shows the number of particles N . The next two columns show the results if the particles are not confined to the droplet interface, both before and after minimizing M_2 . The fourth and fifth column show the configurations resulting from fixing the particles to the droplet interface. The last column shows the experimental results. The letters denote structures that are the same for the same cluster size. The scale bar is 2 μm .

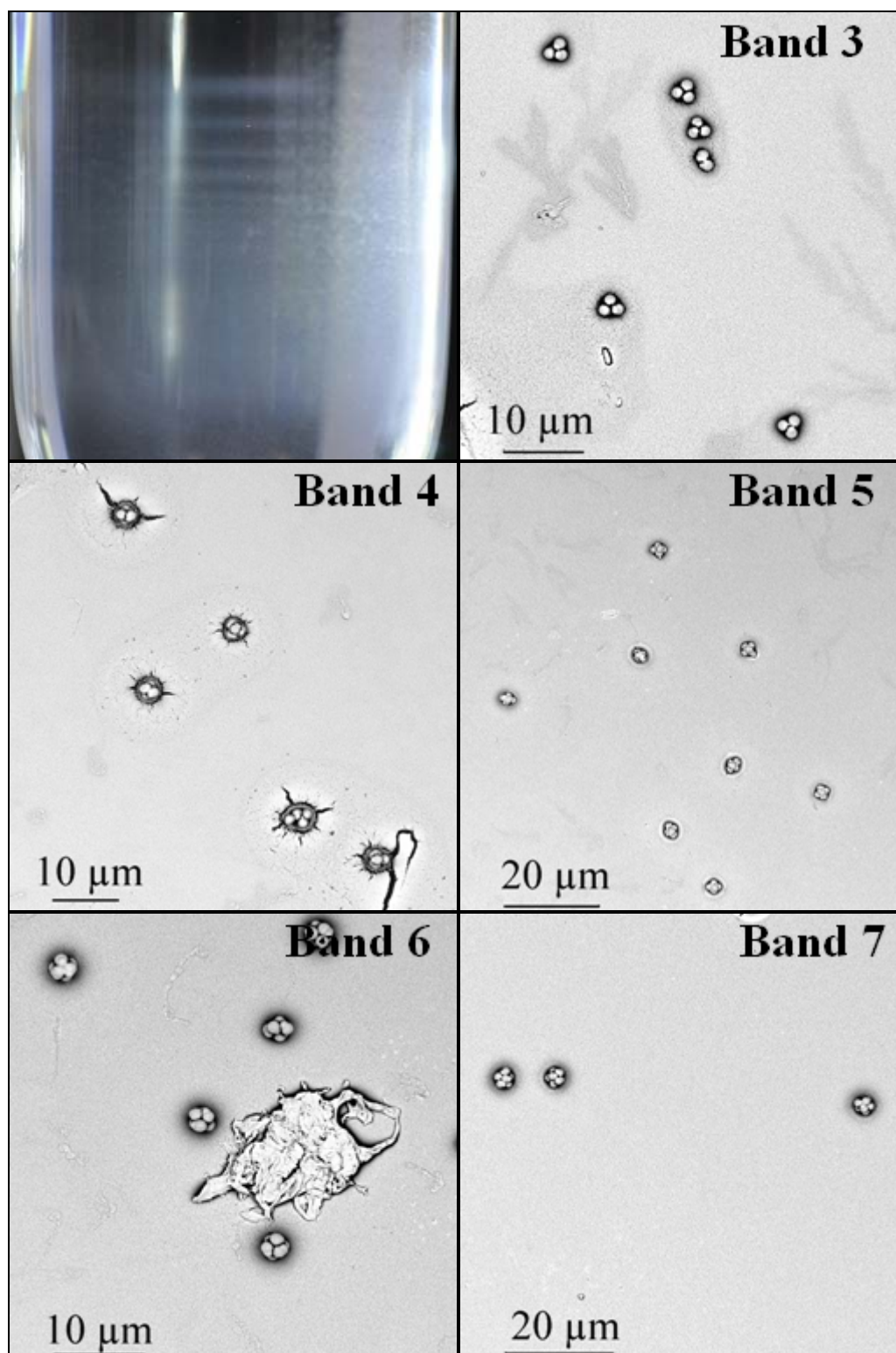
Density Gradient Separation

Clusters from Symmetric Dumbbells



Supplementary Figure 3. The density gradient separation of the clusters applied to clusters of symmetric dumbbells. The top left image is the tube containing the distinct bands of cluster with a given N . The others are SEM images of different bands.

Clusters from Asymmetric Dumbbells



Supplementary Figure 4. The density gradient separation of the clusters of asymmetric dumbbells. The top left image is the tube containing the distinct bands of cluster with a given N . The rest are SEM images of different bands.

Supplementary References

- [1] B. Peng, E. van der Wee, A. Imhof, A. van Blaaderen, *Langmuir* **2012**, 28, 6776.
- [2] B. Peng, H. R. Vutukuri, A. van Blaaderen, A. Imhof, *J. Mater. Chem.* **2012**, 22, 21893.
- [3] M. E. Leunissen, A. van Blaaderen, A. D. Hollingsworth, M. T. Sullivan, P. M. Chaikin, *Proc. Natl. Acad. Sci. USA* **2007**, 104, 2585.
- [4] M. E. Leunissen, J. Zwanikken, R. van Roij, P. M. Chaikin, A. van Blaaderen, A. *Phys. Chem. Chem. Phys.* **2007**, 9, 6405.
- [5] O. D. Velev, A. M. Lenhoff, E. W. Kaler, E. W. *Science* **2000**, 287, 2240.